
Preface

This book provides current information on the development of microfluidics, nanotechnologies, and physical science techniques for the separation, detection, manipulation, and analysis of biomolecules, and should be useful to a wide audience, including molecular and cell biologists, biochemists, microbiologists, geneticists, and medical researchers. Chapters cover a variety of topics and techniques ranging from lab-on-chip technologies and microfluidics-coupled mass spectrometry for separation and detection of biomolecules, including proteins and nucleic acids, to manipulating and probing biomolecules with nanopores, nanochannels, optical, and other physical means, with the possibility of isolation and analysis of individual biomolecules from a single cell, and to structural and functional analysis of biomolecules with liquid nuclear magnetic resonance, X-ray and neutron scattering techniques. The book presents emerging nanotechnologies including quantum dots and molecular fluorescence for imaging and tracking of biomolecules and nanotechnologies for biomolecular delivery, gene therapy, and gene-expression control. Each chapter describes a specific technology with its fundamental mechanism and practical applications for a particular subject area, so that a competent scientist who is unfamiliar with the technology can understand its capabilities and basic procedures. In many cases, a reader should be able to carry out the techniques successfully at the first attempt by simply following the detailed practical procedures (protocols) and/or information (including useful notes) provided in the book. For sophisticated technologies such as neutron scattering, the book describes their physical concepts and discusses the new opportunities that these new technologies may bring for both basic and applied research in the fields of molecular biology and biotechnology. This book consists of 41 chapters that are organized into four parts. The chapters were contributed by nearly 100 authors worldwide, who are among the world's prominent scientists in their fields.

The first half of the volume covers microfluidic and physical methods of bioanalysis. It consists of Part I on applications of microfluidics and nanopores in separation, manipulation, detection, and analysis of biomolecules, and Part II on technologies of physical science in detection and analysis of biomolecules. It contains valuable protocols on microfluidics and physical science-related technologies that may benefit the field of molecular biology. Chapter topics are briefly described below.

Part I consists of Chaps. 1–10: Chap. 1 describes a commercially available nanoflow analytical technology conducted on a microfabricated chip that allows for highly efficient HPLC separation and superior sensitivity for MS detection of complex proteomic mixtures; Chaps. 2–4 describe fabrication of nanofluidic channels for manipulation of DNA molecules, a single-molecule barcoding system using nanoslits for DNA analysis, and microfluidic devices with photodefinable pseudovalves for protein separation, respectively; Chap. 5 introduces specific antibody detection by using a microbead-based assay with quantum dot (QD) fluorescence on a microfluidic chip; Chap. 6 describes a biomolecular sample-focusing method based on a device design incorporating arrays of addressable on-chip microfabricated electrodes that can locally increase the concentration of DNA

in solution by electrophoretically sweeping it along the length of a microchannel; Chap. 7 describes a solid-state nanopore technique for detecting individual biopolymers, and Chap. 8 reports a method of inserting and manipulating DNA in a nanopore with optical tweezers; Chaps. 9 and 10 describe techniques of forming an α -hemolysin nanopore for single-molecule analysis and for nanopore force spectroscopy of DNA duplexes.

Part II consists of Chaps. 11–22: Chap. 11 describes an electrochemical method for quantitative chemical analysis of neurotransmitter release from single cells; Chaps. 12–14 introduce techniques for trapping and detection of single molecules in water, ZnO nanorods as an intracellular sensor for pH measurements, and analysis of biomolecules using surface plasmons; Chap. 15 reports use of residual dipolar couplings in structural analysis of protein–ligand complexes by solution NMR spectroscopy; Chaps. 16 and 17 report Raman-assisted X-ray crystallography for the analysis of biomolecules and methods and software for diffuse X-ray scattering from protein crystals, and Chaps. 18–20 describe deuterium labeling for neutron structure–function–dynamics analysis, the basics and instrumentation of small-angle neutron scattering for molecular biology, and small-angle scattering and neutron contrast variation for studying biomolecular complexes, respectively; Chap. 21 describes the application of tandem mass spectrometry to identification of protein biomarkers of disease, and Chap. 22 describes the use of hyphenated MS techniques for comprehensive metabolome analysis.

The second half of the volume covers nanotechnologies for biosystems, and consists of Part III on applications of quantum dots and molecular fluorescence in detection, tracking, and imaging of biomolecules, and Part IV on nanotechnologies for biomolecular delivery, gene therapy, and expression control. It contains valuable information on nanoscience-empowered molecular biotechnologies.

Part III consists of Chaps. 23–32: Chaps. 23–25 describe multicolor detection of combed DNA molecules using quantum dots, quantum dot molecular beacons for DNA detection, and a gel electrophoretic blotting technique for identifying quantum dot–protein/protein–protein interactions; Chaps. 26 and 27 present techniques for in vivo imaging of quantum dots and efficient biolabels in cancer diagnostics, respectively; Chap. 28 describes monitoring and affinity purification of proteins using dual tags with tetracysteine motifs, and Chap. 29 reports use of genomic DNA as a reference in DNA microarray analyses; Chap. 30 describes single-molecule imaging of fluorescent proteins expressed in living cells; Chap. 31 describes micropositron emission tomography (PET), single-photon emission computed tomography (SPECT), and near-infrared (NIR) fluorescence imaging of biomolecules in vivo, which could lead to a number of exciting possibilities for biomedical applications, including early detection, treatment monitoring, and drug development; Chap. 32 reports a revolutionary photo-based imaging technology: the ultrahigh resolution imaging of biomolecules by fluorescence photoactivation localization microscopy (FPALM) that can now image molecular distributions in fixed and living cells with measured resolution better than 30 nm, which likely represents a breakthrough technology that has now shattered the classic limit of light microscopy resolution associated with the wavelength-dependent light diffraction barrier, thought to be unbreakable for more than 100 years.

In Part IV, Chaps. 33–41 describe nanotechnologies with potential biomedical applications. Specifically, Chap. 33 describes real-time imaging of gene delivery and expression with DNA nanoparticle technologies and Chap. 34 reports nanoparticle-mediated gene delivery. Chapters 35 and 36 describe magnetic nanoparticles for local drug delivery using magnetic implants and functionalized magnetic nanoparticles as an in vivo delivery

system, and Chap. 37 reports formulation/preparation of functionalized nanoparticles for in vivo targeted drug delivery; Chap. 38 reports detection of mRNA in single living cells using atomic force microscopy nanoprobe; Chap. 39 describes a gene transfer technique through reverse transfection using gold nanoparticles; Chap. 40 presents custom-designed molecular scissors for site-specific manipulation of the plant and mammalian genomes, and Chap. 41 describes a technique for determining DNA sequence specificity of natural and artificial transcription factors by cognate site identifier analysis, both of which could lead to modern applications in molecular biology and biomedicine.

Oak Ridge, TN

*James Weifu Lee
Robert S. Foote*

Chapter 2

Nanofluidic Channel Fabrication and Manipulation of DNA Molecules

Kai-Ge Wang and Hanben Niu

Summary

Confining DNA molecules in a nanofluidic channel, particularly in channels with cross sections comparable to the persistence length of the DNA molecule (about 50 nm), allows the discovery of new biophysical phenomena. This sub-100 nm nanofluidic channel can be used as a novel platform to study and analyze the static as well as the dynamic properties of single DNA molecules, and can be integrated into a biochip to investigate the interactions between protein and DNA molecules. For instance, nanofluidic channel arrays that have widths of approximately 40 nm, depths of 60 nm, and lengths of 50 μm are created rapidly and exactly by a focused-ion beam milling instrument on a silicon nitride film; and the open channels are sealed with anodic bonding technology. Subsequently, lambda phage DNA (λ -DNA; stained with the fluorescent dye, YOYO-1) molecules are introduced into these nanoconduits by capillary force. The movements of the DNA molecules, e.g. stretching, recoiling, and transporting along channels, are studied with fluorescence microscopy.

Key words: Nanofluidic channels, Nanopore, Focused-ion beam, DNA molecules, Fluorescence microscopy

1. Introduction

Recently, with the advancements of nanotechnologies, many scientists in different research areas, including both fundamental studies and applied techniques, have focused their attention on the fabrication of nanofluidic devices and the applications in the research of single biomolecules, such as DNA and protein molecules (1–3). Nanofluidic channels with critical dimensions comparable to the size of molecules provide new possibilities for direct observation, manipulation, and analysis of single biomolecules, and

provide a novel technological platform as an ultrasensitive and high-resolution sensor for studying single DNA molecules.

The nanofluidic channel is defined as a channel with at least one cross-section dimension (depth or diameter) in the nanometer range (one-dimension or two-dimension nanochannel) (4). In particular, a nanopore is thought of as a channel with all three dimensions in the nanoscale range, so that the work done with a nanopore falls under the realm of nanofluidics. The potential application of nanopores as detectors for ultrafast genome sequencing is its most attractive application (5–7). Nanofluidics has great benefits for bioscience studies (8), the practical applications of nanofluidics are improvements to the state of the art of DNA separation and sequencing providing significant reductions in both time and cost. The small dimensions of the nanoscale structure reduce processing times and the amount of reagents necessary for assay, substantially reducing costs.

At present, different approaches have been undertaken to successfully fabricate nanoscale structures. In general, nanofabrication methods can be divided roughly into two groups (9): top-down and bottom-up methods. Top-down methods start with patterns made on a large scale and reduce their lateral dimensions before forming nanostructures; these methods are mainly adopted by physics scientists. On the other hand, bottom-up methods begin with atoms or molecules to build nanostructures, in some cases, through smart use of self-organization.

Top-down methods can be classified into two categories, that is, optical masked lithography and optical maskless lithography. The focused-ion beam (FIB) milling tool is a maskless lithography technique that can image features on a lithographic surface directly (10). This technique has the advantages of facility and celerity; the patterns created are smooth and can be easily controlled and faithfully reproduced for different applications.

Micro-scale and submicro-scale fluidic channel arrays have been used for studying single biomolecules for many years (11). However, applications with sub-100 nm fluidic channel arrays in biomolecular studies are rarely reported. The limitation is partially caused by the difficulty of fabrication process and metrology (12). In addition, the properties of DNA molecules confined in these fluidic channels and the dynamics of DNA movements under this condition are not well known.

Although there are many possible applications of nanofluidic channels for DNA study, in this chapter, we focus on the manipulation of single DNA molecules, e.g., stretching, recoiling, and transporting. We describe the fabrication of open nanofluidic channel arrays (40 nm width, 60 nm depth) in silicon nitride (Si_3N_4) membrane surfaces using the FIB milling technique and other nanofabrication techniques. Next, we describe the sealing

of these channels with Pyrex glass by the anodic bonding technique; followed by a description of nanoscale channel arrays used to study the properties of single DNA molecules with the help of fluorescence microscopy. DNA molecules (e.g., λ -phage DNA molecules) stained with the fluorescent dye YOYO-1 can be driven to stretch and transport along these open nanoconduits by capillary force, and also to recoil in the enclosed nanoconduits under the force of the electrode field. Because the dimension of the channel is approximately the natural-state DNA molecule persistence length (~ 50 nm) in aqueous buffer, this nanostructured channel can provide an essential new method for detecting and analyzing single DNA molecules. Such nanoconduits can be used as one component of a “lab-on-a-chip” in the manipulating single biomolecules. These nanochannel systems are also expected to find significant applications in medical diagnostic systems.

2. Materials

2.1. Substrates for Nanofluidic Channels

2.1.1. Substrate Silicon Wafers

1. The substrate silicon wafers are 3-inch or 4-inch diameter, *n*-type, 390- μm or 525- μm thick, double-sided mirror-polished, $\langle 100 \rangle$ single crystal oriented standard bare wafers.
2. Pre-clean the wafers with a H_2SO_4 - H_2O_2 (10:1, v/v) mixture at 120°C for 20 min followed by buffered HF (BHF; $\text{NH}_4\text{F}:\text{HF} = 7:1$, v/v) for 2 min at room temperature to remove surface organics and metals.
3. Rinse with doubly deionized water (Millipore S.A., Molsheim, France).
4. Dry with pure nitrogen gas.

2.1.2. Encapsulating Pyrex Glasses

1. Pyrex 7740 borosilicate glass (3-inch or 4-inch; 600- μm thick, Corning Inc., Corning, NY), matched with the substrate silicon wafer used. The surface roughness of glass is less than 1 nm.
2. Pre-clean the glass with a standard solution of H_2SO_4 - H_2O_2 at 120°C for 20 min, and then dip into a solution of buffered HF (BHF; $\text{NH}_4\text{F}:\text{HF} = 7:1$, v/v) for 2 min at room temperature to remove surface organics and metals.
3. Rinse with doubly deionized water (Millipore S.A.).
4. Dry with a stream of pure nitrogen.

2.2. Biophysics Experimental Buffers

1. Tris-EDTA: 10 mM Tris base, 1 mM EDTA, pH 8.0. All buffers are made with 18.2 M water purified through the Milli-Q water Purification System (Millipore).
2. TBE: 45 mM Tris base, 1 mM EDTA, 45 mM boric acid.

2.3. Biomolecule Sample

1. λ -Phage DNA molecules (Sino-American Biotechnology Company, Beijing, China), stored in alcohol at -20°C . The final DNA concentration is $1\ \mu\text{g}/\text{mL}$ in buffer containing 10 mM Tris-HCl, 10 mM NaCl, and 1 mM EDTA (Sigma, St. Louis, MO, USA), pH 8.0 (*see Note 1*).
2. DNA ($1\ \text{ng}/\mu\text{L}$) is stained with $0.25\ \mu\text{M}$ fluorescent dye YOYO-1 (Molecular Probes, Carlsbad, CA, USA) at a ratio of ten base pairs per dye molecule (bp/dye = 10:1), mixing DNA complex molecules with a specific volume of freshly prepared $0.1\ \mu\text{M}$ dye solution (10 mM Tris, 1 mM EDTA buffer, pH 8.0) (*see Note 2*).

3. Methods

Nanofluidics fabrication and applications have now attracted great enthusiasm because of their brilliant prospects. Nanochannel fabrication techniques should be cost-effective and one should be able to control the channel dimensions precisely. With the rapid improvements of nanotechnological manufacturing, four methods are now (normally) used for fabrication of nanofluidics channels, e.g., bulk nanomachining and wafer bonding (13), surface nanomachining (14), buried channel technology (15), and nanoimprinting lithography (16). In general, the bulk nanomachining technique is the preferred approach for nanoscale fabrication. Among the nanomachining techniques, the FIB milling technique has many advantages (17)—it is an extremely versatile technique for making arbitrary micro- and nano-structures with no essentially required preprocessing or postprocessing.

Nanofluidics channels can act as a novel basis for more precisely controlling the behaviors of single DNA molecules when the diameter of the channel is comparable to or less than the persistence length of the DNA molecule (18). At nanoscale dimensions, different biophysical phenomena start to dominate, this leads to new scientific insights and applications (19). We can use these nanoscale structures (open nanofluidic channels and enclosed nanofluidic channels) to manipulate, detect, and analyze individual biological molecules, and can also carry out individual molecular reactions within these nanofluidic environments while electric fields are used to drive flow, move analytes, and separate ionic species.

3.1. Fabrication of Nanofluidic Channels

3.1.1. Creating Free-standing Si_3N_4 Crystal Membranes

1. 500-nm thick lower stress ($\sim 200\ \text{MPa}$ tensile) Si_3N_4 films are deposited on both sides of the prepared bare silicon wafer by standard low-pressure chemical vapor deposition (LPCVD, M80100, Sevenstar Electronics Co., Beijing, China). The working condition are: temperature, 800°C ; pressure, 200 mTorr; gas, SiCl_2H_2 and NH_3 .

2. Approximately 100- μm thick photoresist (ARN7500, GermanTech Co., Beijing, China) is spun onto the front side of the silicon wafer with the spin coater (KW-4A, XiaMen Chemat Scientific Instrument Company, XiaMen, China) at the speed of 5,000 rpm.
3. Bake the wafer at 140°C for approximately 30 min and then store at room temperature in a dust-free environment.
4. A standard photolithography process is used to pattern an appropriate square ($\sim 1,200 \times 1,200 \mu\text{m}^2$) in the photoresist layer, that is, the same square pattern is exposed on the Si_3N_4 surface.
5. The reactive ion etching (RIE, Plasmalab 80Plus RIE, Oxford Instruments Co., Abingdon, UK) is used to open the hole in the Si_3N_4 membrane with a SF_6/O_2 (1:4, v/v) gas mixture for 2 min, working conditions: RF, 100 W; pressure, 110 mTorr; temperature, 100°C.
6. The residual photoresist on the front surface is removed using oxygen plasma with an O_2/CF_4 gas mixture (CF_4 is $\sim 20\%$ in total gas mixture volume); RF power, 60 W; pressure, 135 mTorr; temperature, 120°C.
7. The wafer is immersed into 40% (m/v) potassium hydroxide KOH(aq) at 60°C for ~ 10 min to create a $100 \times 100\text{-}\mu\text{m}^2$ free-standing Si_3N_4 membrane (*see Note 3*).

3.1.2. Fabricating Nanofluidic Channels

1. Vent the FIB (DB235, FEI Company, Hillsboro, OR, USA) system to mount the silicon wafer with a free-standing Si_3N_4 membrane sample carefully and tightly and then pump down the system. When vacuum is reached, switch on the beam. Carefully move the sample in the Z-direction to get closer to the working distance.
2. On the backside of the free-standing Si_3N_4 membrane, a standard FIB milling technique is used to fabricate nanoscale fluidic channel arrays. The model of FIB drilled is single-pass with a 30 keV Ga^+ ion beam. The initial incident ion beam full-width half-maximum (WHFM) diameter is 20 nm.
3. Choose appropriate working conditions to control the channels' depth and width, where ion beam current, overlap, and dwell time are 10 pA, 50%, and 0.3 μs , respectively (*see Note 4*).
4. Deposit platinum in the two reservoirs as the electrode.
5. A wafer bonder (EV501, EV Group, St. Florian, Austria) is used to bond the Pyrex glass to the substrate wafer. The voltage applied on the glass wafer is negative with respect to that of the silicon wafer. The bonding process is approximately 30 min at 350°C with an applied voltage of 800 V. A sketching image of nanofluidic channel fabrication is shown in **Fig. 1**. Some typical nanochannel arrays created are shown in **Fig. 2**.

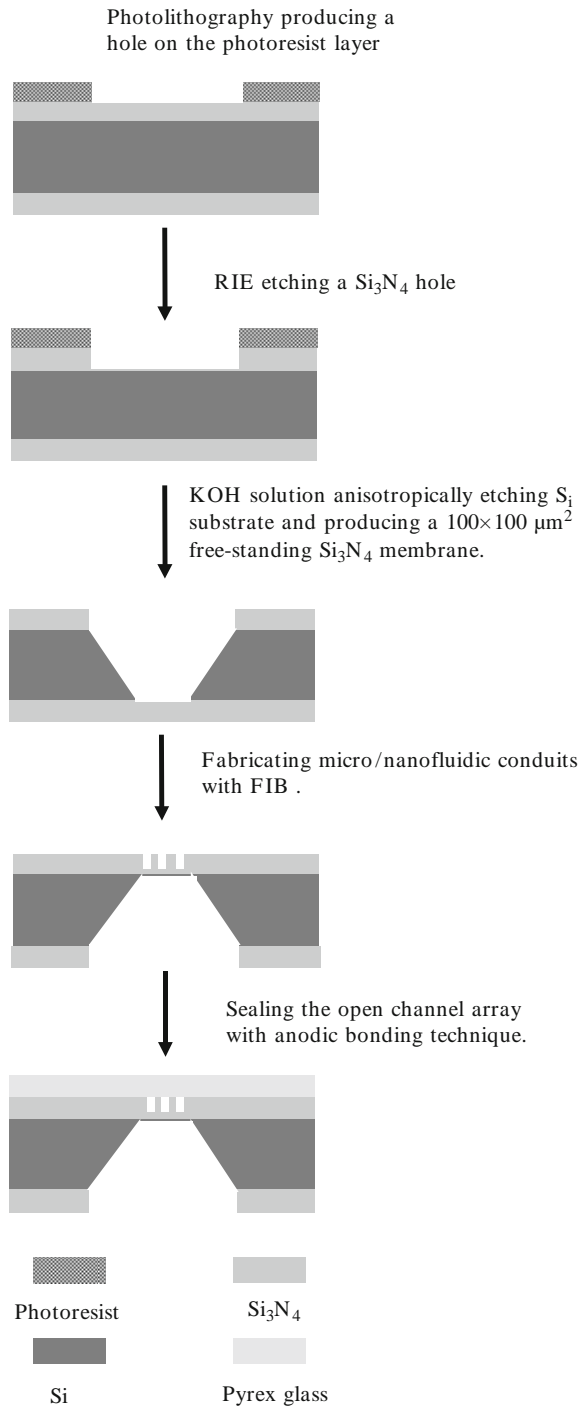


Fig. 1. Schematic drawing of fabricating process for nanofluidic channels.



Fig. 2. SEM images of nanofluidic channel arrays at the center of the free-standing Si_3N_4 membrane.

3.2. Manipulation of DNA Molecules

3.2.1. Preparing Biomolecule Samples

1. Incubate the DNA/YOYO-1 mixture solution in a dark room for ~30 min. In all experiments, the DNA base pair-to-dye ratio is kept at 10:1 (bp/dye = 10).
2. Dilute the DNA/YOYO-1 complex solution to 6.5 pM in a 50 mM Bis-Tris buffer (pH 7.5, Sigma).
3. Admix the buffer with 5% (v/v) β -mercaptoethanol (Sigma) as an antiphotobleaching agent and 2.5% (w/w) poly (*n*-vinylpyrrolidone) (PVP, Sigma) to reduce both electroosmotic flow and nonspecific binding of DNA to channel walls.

3.2.2. *Manipulating DNA Molecules in the Nanofluidic Channels*

1. Carefully place the nanofluidics channel system on the luggage carrier.
2. With a syringe, transfer the DNA/YOYO-1 complex solution into one reservoir of the open fluidic channel system with a Digital Precision Microliter Pipette (Gilson S.A.S., Roissy en France, France). The solution migrates into and is transported along the open channels by capillary action as soon as it arrives at the channel entrance (*see Note 5*).
3. With a syringe, transfer the DNA/YOYO-1 complex solution into one reservoir of the enclosed nanochannel system; the solution is loaded into the nanochannels via capillary action and then transported through the nanochannels by using an applied electrical field with platinum electrodes inserted into the reservoirs.
4. A 5-V bias is applied to drive a DNA molecule from the reservoir into a nanochannel (*see Note 6*).
5. Switch off the bias field before the DNA molecule has completely entered the nanochannel. As a result, DNA molecule is driven back to the reservoir and can be observed to both recoil and unstretch simultaneously.
6. The DNA complex molecule is then driven entirely into the nanochannel, and the bias field is switched off (*see Note 7*).
7. A DNA molecule is electrophoretically driven from the reservoir into a nanochannel. Upon fully entering a nanochannel, the molecule begins to relax and finally reaches its equilibrium extension length inside the channel (*see Note 8*).
8. After the molecule has completely relaxed to its equilibrium length inside the nanochannel, it is electrophoretically driven to the exit of the channels. Once the tip of the molecule is straddling the interface, the voltage is turned off and the molecule is observed to completely recoil from the nanochannel (*see Note 9*).

3.2.3. *Single Molecular Optical Imaging*

1. The fluorescently stained DNA/YOYO-1 complex molecules are observed using an inverted optical microscope (IX-70, Olympus, Tokyo, Japan) by epifluorescence with a 20× objective.
2. A 100-W mercury lamp is used in combination with a U-MWB excitation cube (BP450–480, dm500, BA515) for light-induced fluorescence illumination (*see Note 10*).
3. Fluorescence light from the complex molecules is detected by a cooled charge-coupled device (CCD) camera (1,300 × 1,300 pixels, 12-bit digitization; Cool SNAP-HQ, Roper Scientific, Inc., Tucson, AZ, USA). MetaMorph software (Universal Imaging Corporation, West Chester, PA, USA) is used for the system control, data acquisition, and data processing.

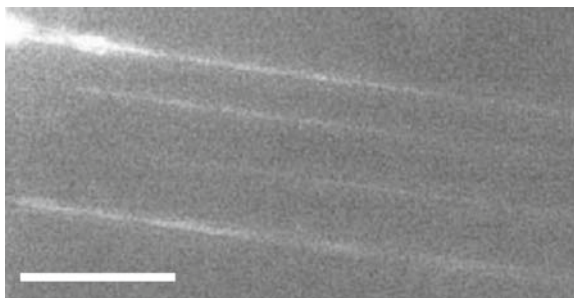


Fig. 3. A typical fluorescence image of stained λ -phage DNA inside fluidic channels. Scale bar, 10 μm .

The CCD acquisition time is 3 s (*see Note 11*). **Figure 3** shows a typical fluorescence image of the λ -phage DNA molecules passing along the open fluidic channels.

4. Notes

1. Lambda-phage DNA is a linear double-stranded helix that contains 48,502 kbp, its molecular mass is ~ 30.6 MDa, and its contour length is ~ 16.2 μm . It is widely used in life sciences.
2. When the mixing ratio (dye molecules per base pair) is below 1:8, the predominant binding mode of YOYO-1 on DNA is bis-intercalation; when the mixing ratio is above 1:8, groove association (external binding) with DNA begins to contribute significantly.
3. When the wafer is immersed into the KOH solution, the silicon is etched at 54.7-degree angles relative to the surface normal. This anisotropic etching creates a free-standing 100×100 μm^2 Si_3N_4 membrane on the backside of the wafer.
4. These open nanochannels can be made with different shapes, e.g., uniform-linear or curvilinear. All of these nanochannels are combined by two bigger containers, which act as the solution reservoirs. The linear nanofluidic channel can be created down to 40-nm width and 60-nm depth. The channel lengths are 50 μm , and the distance between two channels is 5 μm .
5. λ -phage DNA molecules can be observed stretched and threaded along these open nanochannels. DNA molecules can be moved along the channels, although they move only a short distance, not through the whole conduit. In addition, it can be seen that not all channels are filled with DNA

molecules, i.e., there is only buffer liquid within some conduits.

6. This bias resulted in $E = 100$ V/cm in the nanochannels, which is large enough to drive DNA molecules. DNA molecules carry negative charges, which prevent them from adhering to the nanofluidic channel walls, which are also negatively charged. This electrostatic repulsion effectively prevents the nonspecific binding of biomolecules to the nanofluidic channel surface.
7. Once the DNA molecule has contracted, it is slowly driven back down the nanochannel until a small portion of the molecule has reached the reservoir. At this point, the field is switched off and the molecule is observed to undergo a pure recoil process.
8. Stretching is caused by the electric force pulling the molecules into the nanochannel against a resistance at the entrance. The resistance at the entrance is probably caused by the entropic interface force and friction for molecules encountering the entrance edges.
9. Because molecules are allowed to reach equilibrium before beginning to recoil, this process is driven purely by the entropic recoil force and unaffected by elastic restoration.
10. YOYO-1 has an excitation maximum at 491 nm and an emission maximum at 509 nm; that is, YOYO-1 molecules emit green fluorescence under the excitation of blue light.
11. YOYO-1 molecules bind strongly to doubled-strand DNA molecules and the fluorescence quantum yields of the bound dyes are very high. The amount of intercalated dye is proportional to the length of the molecule, therefore, measuring the total fluorescent intensity from a single molecule gives a direct measurement of its length.

Acknowledgments

This work is supported by grants from the National Natural Science Foundation of China (No. 60771048, No. 60025516, and No. 10334100), and the Major Project of National Science Foundation of China (No. 60138010), and partly supported by National Center for Nanoscience and Technology, China.

References

1. Tegenfeldt, J. O., Prinz, C., Cao, H., Huang, R. L., Austin, R. H., Chou, S. Y., Cox, E. C., Sturm, J. C., (2004) Micro- and nanofluidics for DNA analy. *Anal. Bioanal. Chem.* **378**, 1678–1692
2. van der Heyden, F. H. J., Stein, D., Dekker, C. (2005) Streaming currents in a single nanofluidic channel. *Phys. Rev. Lett.* **95**, 116104
3. Baldessari, F. and Santiago, J. G. (2006) Electrophoresis in nanochannels: brief review and speculation. *J. Nanobiotechnology.* **4**, 12–16
4. Eijkel, J. C. T. and van den Berg, A. (2005) Nanofluidics: what is it and what can we expect from it? *Microfluid Nanofluids.* **1**, 249–267
5. Henrickson, S. E., Misakian, M., Robertson, B., Kasianowicz, J. J. (2000) Driven DNA transport into an asymmetric nanometer-scale pore. *Phys. Rev. Lett.* **85**, 3057–3060
6. Li, J., Stein, D., McMullan, C., Branton, D., Aziz, M. J., Golovchenko, J. A. (2001) Ion-beam sculpting at nanometre length scales. *Nature.* **412**, 166–169
7. Dekker, C. (2007) Solid state nanopores. *Nat. Nanotechnol* **2**, 209–215
8. Lin, Y., Huang, M., Chang, H. (2005) Nanomaterials and chip-based nanostructures for capillary electrophoretic separations for DNA. *Electrophoresis.* **26**, 320–330
9. Mijatovic, D., Eijkel, J. C. T., van den Berg, A. (2005) Technologies for nanofluidic systems: top-down vs. bottom-up. *Lab. Chip.* **5**, 492–500
10. Biance, A. L., Gierak, J., Bourhis, E., Madouri, A., Lafosse, X., Patriarche, G., Oukhaled, G., Ulysse, C., Galas, J. C., Chen, Y., Auvray, L. (2006) Focused ion beam sculpted membranes for nanoscience tooling. *Microelectro. Eng.* **83**, 1474–1477
11. Squires, T. M. and Quake, S. R. (2005) Microfluidics: fluid physics at the nanoliter scale. *Rev. Mod. Phys.* **77**, 977–1025
12. Stein, D., van der Heyden, F. H. J., Koopmans, W. J. A., Dekker, C. (2006) Pressure-driven transport of confined DNA polymers in fluidic channels. *Proc. Natl. Acad. Sci. U.S.A.* **103**, 15853–15858
13. Cao, H., Yu, Z. N., Wang, J., Tegenfeldt, J. O., Austin, R. H., Chen, E., Wu, W., Chou, S. Y. (2002) Fabrication of 10 nm enclosed nanofluidic channels. *Appl. Phys. Lett.* **81**, 171–176
14. Ahpan, H., Mondin, G., Hegelbach, N. G., de Roij, N. F., Staufer, U. (2006) Filling kinetics of liquids in nanochannels as narrow as 27 nm by capillary force. *J. Colloid Interface Sci.* **293**, 151–157
15. de Boer, M. J., Tjerkstra, R. W., Berenschot, J. W., Jansen, H. V., Burger, G. J., Gardniers, J. G. E., Elwenspoek, M., van den Berg, A. (2000) Micromachining of buried micro channels in silicon. *J. Microelectromech. Syst.* **9**, 94–103
16. Guo, L. J., Cheng, X., Chou, C. (2004) Fabrication of size controllable nanofluidics channels by nanoimprinting and its applications for DNA stretching. *Nano. Lett.* **4**, 49–73
17. Yanagi, H. and Kwawi, Y. (2004) Organic field effect transistor with narrow channel fabricated using focused ion beam. *J. Appl. Phys.* **43**, L1575–L1577
18. Craighead, H. G. (2000) Nanoelectromechanical systems. *Science.* **290**, 1532–1535
19. Mannion, J. T., Reccius, C. H., Cross, J. D., Craighead, H. G. (2006) Conformational analysis of single DNA molecules undergoing entropically induced motion in nanochannels. *Biophys. J.* **90**, 4538–4546